LIGHTCURVES OF EIGHTEEN ASTEROIDS

Eric V. Dose
3167 San Mateo Blvd NE #329
Albuquerque, NM 87110
mp@ericdose.com

(Received: 2021 Jan 13, Revised: 2021 Mar 3)

Using a previously described workflow built on applying to each image dozens of comparison stars from the ATLAS refcat2 catalog, we have obtained and present here lightcurves and synodic rotation periods for eighteen asteroids.

Introduction and Workflow Description

In this paper we present asteroid lightcurve photometry results achieved by following the workflow process described by Dose (2020a). This workflow applies to each image an ensemble of typically 30-150 ATLAS refcat2 catalog (Tonry et al, 2018) comparison ("comp") stars for yielding photometric solutions. Diagnostic plots and this large number of comp stars allow for effective identification and removal of outlier, variable, and poorly measured comp stars. Improved handling of atmospheric extinction was described previously in Dose (2020b).

The present workflow produces a raw lightcurve, that is, the best estimates of asteroid magnitude on catalog basis (here, Sloan r'), unreduced and without H-G adjustment. These magnitudes are imported directly into *MPO Canopus* software (Warner, 2018) where they are adjusted for distances and phase-angle dependence, fit by Fourier analysis including identifying and ruling out of aliases, and plotted. Phase-angle dependence is corrected with a H-G model, using $G = 0.15$ for each asteroid unless otherwise specified.

No nightly zero-point adjustments (DeltaComps in *MPO Canopus* terminology) were made to any session herein, other from adjusting the G value (H-G). All lightcurve data herein have been submitted to ALCDEF.

Over the past few months, minor improvements have been made to the workflow. In nightly planning, we now superimpose a Digital Sky Survey photo on each asteroid's predicted path; observations are suspended (and imaging time is released to other asteroids) during any time periods where a given asteroid will be too near any background star. We use *TheSkyX* software, build 12868 (Software Bisque) to make these overlays and to predict accurate times of asteroid proximity to background stars. While this practice is laborious, it has practically eliminated rejection of images for background star interference. The occasional fragmentation of sessions is unwelcome, but if stars do lie in the asteroid's path, this fragmentation is already unavoidable, and accounting for this during planning minimizes lost observing time.

When imaging, we now make longer image exposures to improve the resulting lightcurves, even at the cost of lower image frequency. The application of very many comp stars has beaten down errors in comp-star flux and zero-point to the extent that asteroid photometric errors themselves entirely dominate errors in final magnitudes.

For deciding when to close a given asteroid's observing campaign, elimination of need to make nightly zero-point adjustments has reduced the closing criteria to only two: (1) absence of any phase-plot gap significant enough to risk fit by exclusion, and (2) absence of any remaining credible alias in the best period spectrum — or a recognition that aliases cannot be eliminated within the remaining nights of the current apparition.

Lightcurve Results

Eighteen asteroids were observed from Deep Sky West observatory (IAU V28) at 2210 meters elevation in northern New Mexico. Images were acquired with a 0.35-m SCT reduced to f/7.7; a SBIG STXL-6303E camera cooled to -35C and fitted with a Clear filter (Astrodon); and a PlaneWave L-500 direct-drive mount. The equipment was operated remotely via ACP software version 8.3 (DC-3 Dreams), running plan text files generated for each night by the author's python scripts (Dose, 2020a). Observations often cycled between 2-4 asteroids, as facilitated by the mount's rapid slews. Exposure times targeted 5-8 millimagnitudes uncertainty in asteroid raw magnitude, subject to a maximum of 900 seconds and a minimum of 90 seconds to ensure suitable comp-star photometry. All exposures were autoguided.

FITS images were plate-solved by *PinPoint* (DC-3 Dreams) or *TheSkyX* and were calibrated using temperature-matched, median-averaged dark images and recent flat images of a flux-adjustable flat panel. Every photometric image was visually inspected; all images with poor tracking, obvious interference by cloud or moon, or having stars or other light sources within 10 arcseconds of the target asteroid were excluded. Photometry-ready images that pass these screens were submitted to the workflow, which applies separately measured second-order transforms from Clear filter to deliver asteroid magnitudes in Sloan r' passband.

Errors are given in parentheses after the value and are in units of the last decimal place.

589 Croatia. Aliases have afflicted previous synodic period determinations for this bright outer main-belt asteroid. Reports of 11.7 h (Warner, 2008), 16.384 h (Waszczak et al, 2015), 24.821 h (Behrend, 2013web) and 24.734 h (Mas et al, 2018) have LCDB quality codes of 2+ or lower; the two phase plots in these reports contain significant gaps.

We report a period of 24.933(2) h from a clearly bimodal lightcurve taken over eight weeks. The previously reported period of 16.384 h is an alias by one-half period per 24 hours. A G value (H-G phase correction) of 0.10 improved the Fourier fit; our RMS error (observations vs best Fourier fit) is 8 millimagnitudes.

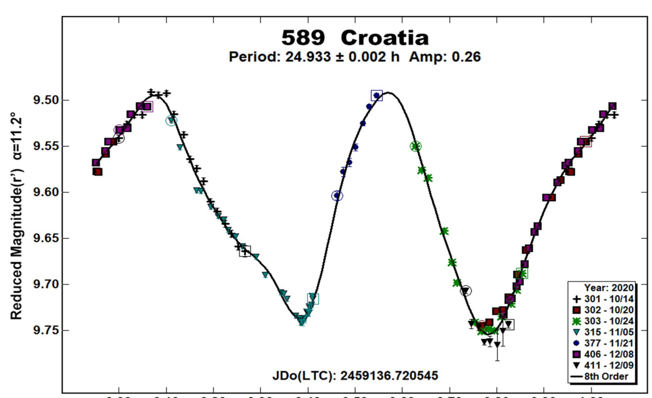

Number	Name	yyyy mm/dd		Phase	L_{PAB}	B_{PAB}	Period(h)	P.E.	Amp	A.E.	Grp
589	Croatia	2020	10/14-12/09	*11.3,10.6	50	-11	24.933	0.002	0.26	0.02	MB-O
722	Frieda	2020	10/30-11/22	12.6,1.1	60	2	128.990	0.176	0.71	0.04	FLOR
805	Hormuthia	2020	10/09-11/14	12.6,19.5	347	-3	11.890	0.002	0.10	0.03	UKN
866	Fatme	2020	11/12-12/23	*6.9,8.9	67	-4	11.600	0.001	0.19	0.03	MB-O
1114	Lorraine	2020	10/20-11/14	3.0,12.1	20	-2	20.680	0.005	0.10	0.02	MB-O
1241	Dysona	2020	10/02-10/16	15.8,14.1	65	26	8.606	0.002	0.36	0.02	MB-O
1721	Wells	2020	10/16-11/06	*8.2,8.1	34	19	11.845	0.001	0.08	0.03	MB-O
2689	Bruxelles	2020	10/18-11/20	*8.2,8.5	41	-4	101.800	0.026	0.80	0.03	FLOR
3001	Michelangelo	2020	10/18-10/23	14.4,15.4	13	24	8.345	0.002	0.26	0.02	MB-I
3600	Archimedes	2020-21	12/24-01/12	18.3,11.3	130	9	5.436	0.001	0.22	0.03	MB-I
4717	Kaneko	2020-21	11/20-01/03	12.4,19.2	28	-8	12.811	0.001	0.23	0.02	EOS
4995	Griffin	2020	10/31-12/06	33.8,24.3	84	30	26.370	0.002	0.74	0.03	MC
5802	Casteldelpiano	2020	11/22-12/06	1.8,9.3	58	2	2.971	0.001	0.18	0.04	FLOR
8078	Carolejordan	2020	10/21-10/24	6.9,8.6	18	-2	3.054	0.001	0.38	0.02	MB-I
10221	Kubrick	2020	10/24-12/22	*12.9,15.1	58	2	11.070	0.002	0.20	0.06	V
21787	1999 SG4	2020-21	12/07-01/08	7.1,18.5	60	4	2.939	0.001	0.20	0.03	EUN
26858	Misterrogers	2020	10/11-11/17	12.8,28.4	2	6	6.054	0.001	0.14	0.03	MC
49125	1998 SB22	2020	11/06-12/04	2.0,13.8	42	-4	5.968	0.001	0.64	0.10	V

Table I. Observing circumstances and results. The phase angle is given for the first and last date. If preceded by an asterisk, the phase angle reached an extrema during the period. L_{PAB} and B_{PAB} are the approximate phase angle bisector longitude/latitude at mid-date range (see Harris et al., 1984). Grp is the asteroid family/group (Warner et al., 2009).

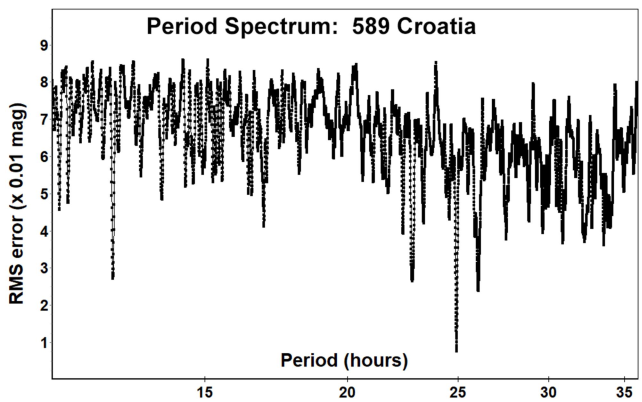

722 Frieda. Two recent previous period determinations for this Flora-family asteroid yielded 131.1 h (Polakis, 2019) and 30.06 h (Olguín et al, 2020). We generally confirm the longer period with a determination of 128.99(18) h, although we observed a much larger amplitude of 0.71 magnitudes than given by either previous report.

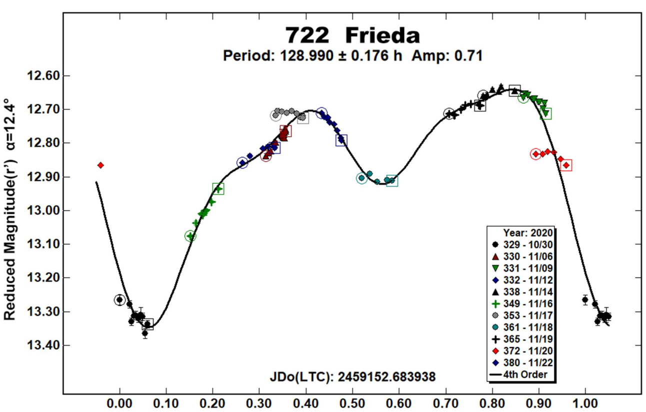

Two nights' observations of 722 Frieda (near phases 0.36 and 0.92) showed small, systematic intra-night deviations from the best Fourier fit, possibly indicating a modest effect from tumbling. The Asteroid Lightcurve Database (LCDB, Warner et al, 2009) entry for 722 Frieda also suggests tumbling, which would not be surprising given the long period. A *G* value of 0.40 markedly improved the Fourier fit vs *G* of 0.15; RMS error is 32 millimagnitudes.

805 Hormuthia. A convincing rotation period for this large (67 km) asteroid of undetermined family has proven difficult to obtain (Polakis, 2019), surely due to its low amplitude, very simple lightcurve shape with only a single broad feature, as well as an orbit of low eccentricity that precludes close approaches to earth. Periods of 9.510 h (Pilcher and Benishek, 2009), 23.76 h (Behrend 2019web), and 35.64 h (Polakis, 2020) have been reported. We find a period of 11.890(2) h from observations assisted by a rather bright 2020 apparition, though the target's declination was unfavorable for the observer's site. RMS error is 8 millimagnitudes.

A small gap in our phase plot was unavoidable as the period is quite close to one-half sidereal day (11.967 h). Its unfavorable declination for the observation site also prevented observing sessions longer than about one-half period. Even so, the present lightcurve shape is clear, when taken on the proposed monomodal basis.

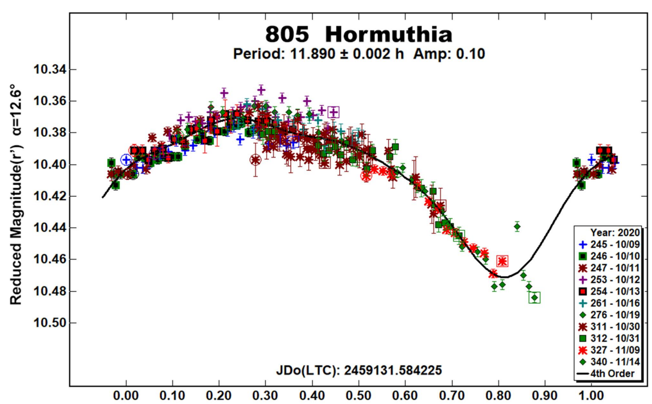

The 9.510 h period listed as favored in the LCDB is an alias of the present result, differing by exactly one-half period per 24 hours; it simply does not appear in our period spectrum. Similarly, the previous report of 23.76 h differs by exactly one period per 24 hours; the reported trimodal period of 35.64 h is quite close to three times the present monomodal solution, and it cannot be ruled out. Our period spectrum does show the expected minor aliases near 6, 8, and 16 h, but these candidate periods give poor Fourier fits to our photometric data, so we exclude them. In the end, we adopt the monomodal 11.890 h solution, though bimodal and even trimodal solutions also possible.

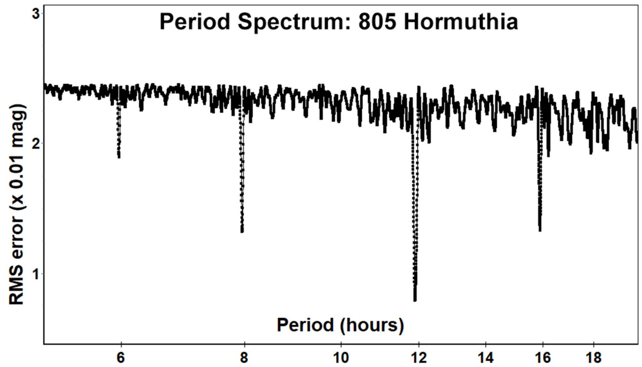

866 Fatme. Our period determination of 10.600(1) h for this outer main-belt asteroid differs from previous reports known to the author: 5.800 h (Polakis, 2018), 9.4 h (Behrend, 2004web), 9.36 h (Behrend, 2012web), 20.03 h (Stephens, 2002), and 20.07 h (Aznar Macias et al, 2016). Our lightcurve is bimodal, and our period estimate is twice that of Polakis' monomodal solution. The period estimates of 9.4 h and 9.36 hours are aliases of our estimate by one half-period per 24 hours. A G value of 0.18 improved the Fourier fit over G of 0.15. RMS error is 9 millimagnitudes.

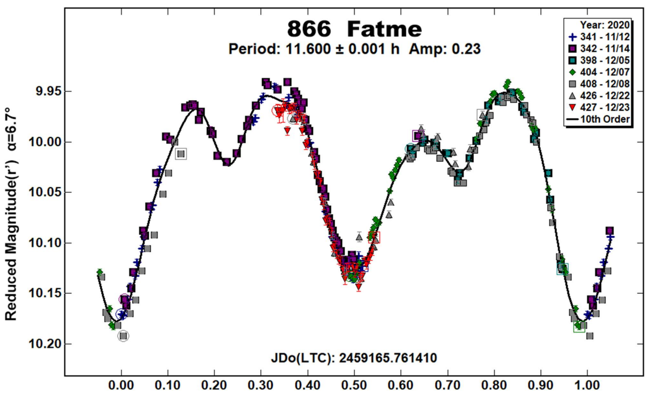

1114 Lorraine. Our synodic rotation period of 20.680(5) h confirms a previous report of 20.7 h (Ditteon et al, 2018) but differs from an earlier report of 32 h (Behrend, 2005web); the latter is entirely absent from our period spectrum. Given the relatively low amplitude and monomodal shape of the lightcurve, our observations emphasized the rapid brightening near phase 0.8-0.95, in an effort to rule out aliases and to sharpen the period estimate. RMS error is 8 millimagnitudes.

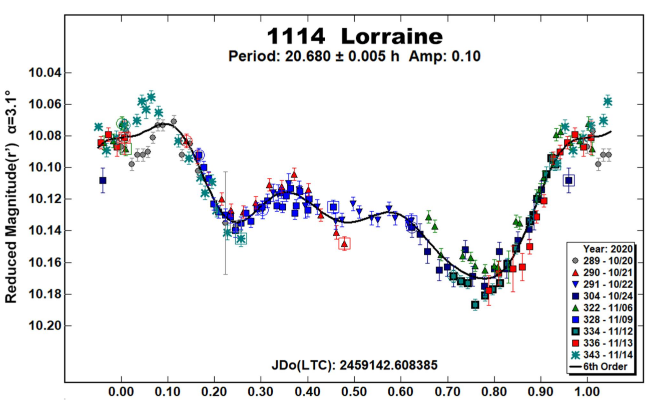

1241 Dysona. The 2020 apparition of this large outer main-belt asteroid offered a new phase angle bisector for shape studies, as well as a declination unusually advantageous for the author's observing site. The period was determined as 8.606(2) h, confirming all known previous reports of 8.61 h (Behrend, 2002web), 8.6080 h (Oey et al, 2007), 8.60738 h (Hanuš et al, 2013), and 8.6092 h (Behrend, 2019web). A *G* value of 0.05 slightly improved the Fourier fit over the default value of 0.15. RMS error is 12 millimagnitudes.

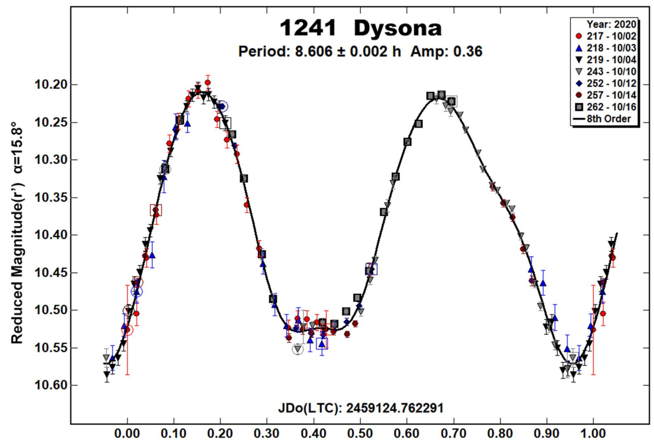

1721 Wells. No previous lightcurve or period reports are known for this outer main-belt asteroid. The 2020 apparition was at advantageous declinations for our observing site, which afforded long observing sessions to help overcome the period's proximity to one-half day. The synodic period determined here is 11.845(1) h. RMS error was 9 millimagnitudes.

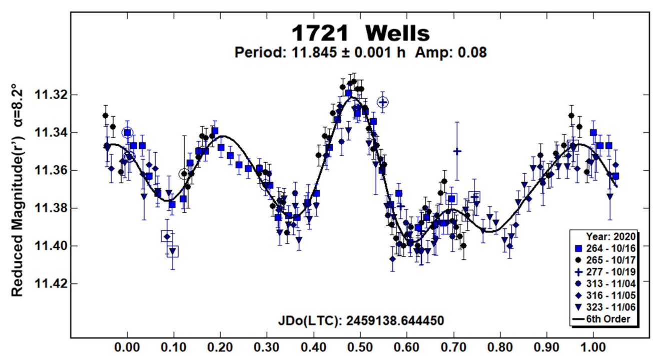

The unusual lightcurve shape, low amplitude, and the period's proximity to one-half day all complicated the *de novo* period search, but the best Fourier fit had low RMS error, and the phase angles ranged less than one degree, effectively removing the need to estimate *G*. The resulting period spectrum appears unambiguous.

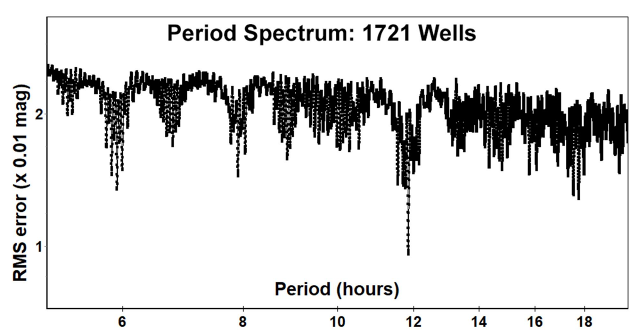

2689 Bruxelles. The previously reported (Hess and Ditteon, 2016) synodic period of 8.71 h and amplitude of perhaps 0.08 magnitude for this Flora-family asteroid were simply not confirmed by data from our first observing sessions. In our surprise, we launched a *de novo* period determination, which converged on 101.80(3) h and amplitude of 0.80 magnitude. RMS error was 19 millimagnitudes.

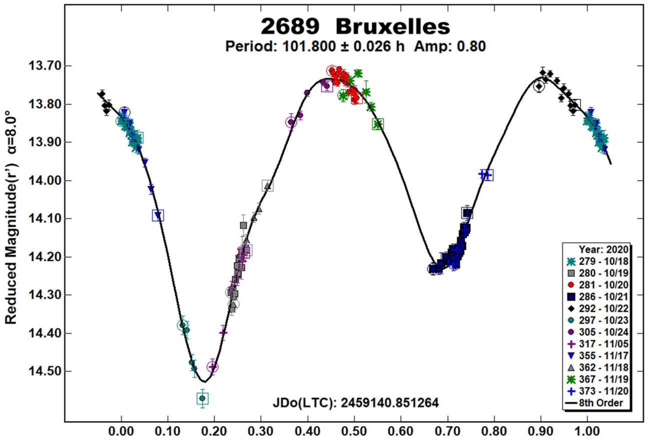

We are confident in our widely differing period estimate — yet both our large amplitude and the small amplitude previously reported could be correct for their observation dates. Our observations' viewing angle (phase angle bisector PAB of 41º, –3º) is very nearly perpendicular to that of the previous observations (PAB 133º, –3º), so it is plausible that in 2020 we observed 2689 Bruxelles near its rotational equator and that in 2015 it was observed near a pole. The favorable 2022 apparition (PAB 201º, 4º) affords a superb opportunity to test this idea, as well as to take data at new viewing angles for shape modeling.

3001 Michelangelo. The synodic rotation period for this inner main-belt asteroid is found to be 8.345(2) h, in agreement with previous reports of 8.338 h (Ditteon et al, 2011), 8.343 h (Waszczak et al, 2015), and 8.35088 h (Pál et al, 2020). A *G* of 0.50 optimized the Fourier fits. RMS error is 11 millimagnitudes.

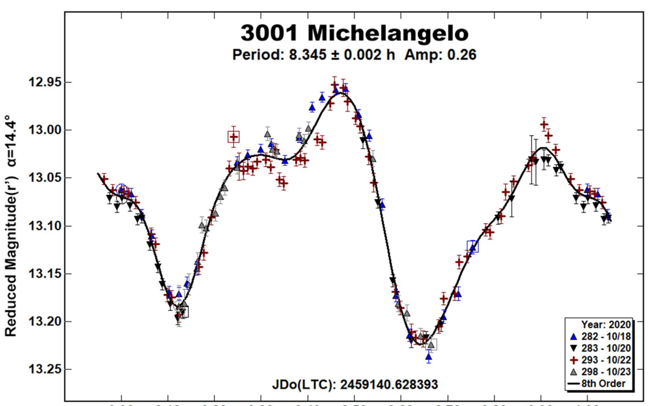

3600 Archimedes. We measure a synodic period for this inner main-belt asteroid as 5.4360(5) h, confirming one previous report of 5.439(1) h (Benishek, 2018). The lightcurve given in that previous report remarkably resembles a time-reversal of the lightcurve given here. A *G* value of 0.45 gave far superior Fourier fits to those with customary *G* of 0.15; RMS error is 16 millimagnitudes.

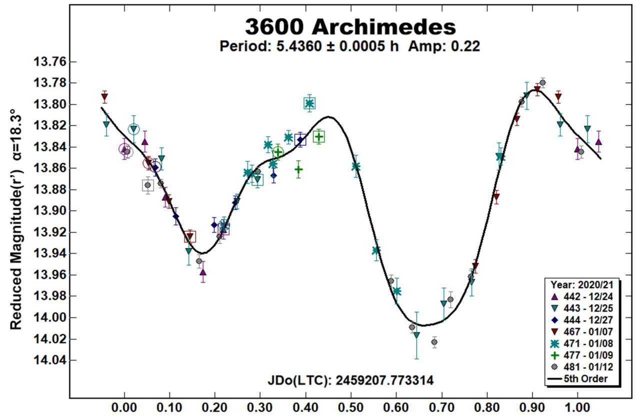

4717 Kaneko. For this Eos-family asteroid, our synodic rotation period of 12.811(1) h confirms two recent reports of 12.7998 h (Pál, 2020) and 12.7082 h (Singh et al, 2020). We estimate a much smaller amplitude (0.23 mag) than does the second report (0.61 mag), and our phase plot is more obviously bimodal. A *G* value of 0.22 improved the Fourier fits over that with *G* = 0.15; RMS error was 13 millimagnitudes.

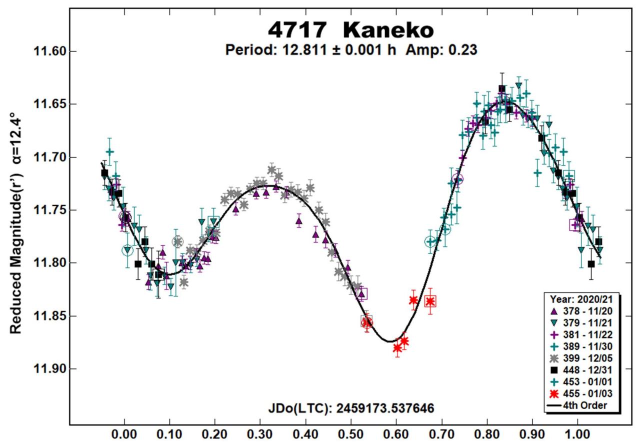

4995 Griffin. This small, high-albedo Mars-crosser was observed near +60º declination for 14 nights during its very favorable 2020 opposition. The period was found to be 26.370(2), in agreement with previous reports of 26.37 h (Warner, 2003, as 1984 QR, partial lightcurve) and 26.3920 h (Ďurech et al, 2016). A *G* value of 0.25 improved Fourier fits over those with *G* = 0.15; RMS error was 14 millimagnitudes.

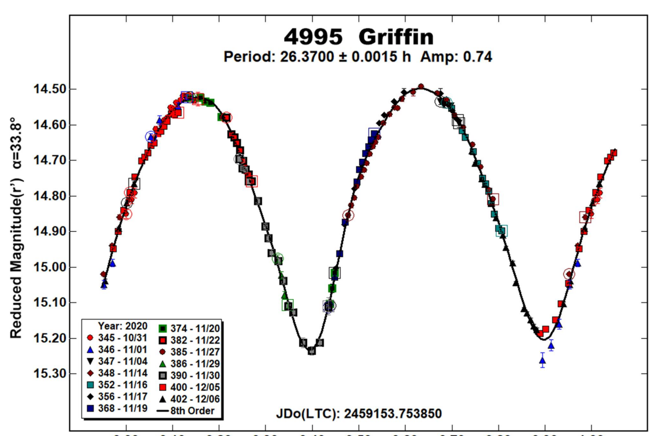

5802 Casteldelpiano. This Flora-family asteroid was detected in images targeting 10221 Kubrick and then was followed in its own right. Our synodic period estimate of 2.9706(2) h confirms previous reports of 2.971 h (Waszczak et al, 2015) and 2.9705 h (Pravec, 2018web). A *G* value of 0.30 markedly improved the Fourier fit over *G* = 0.15; RMS error was 20 millimagnitudes.

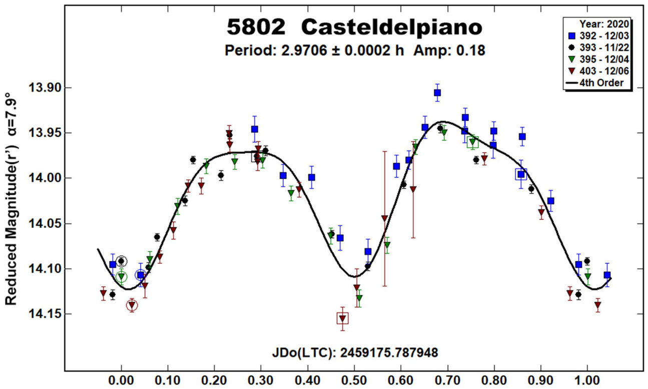

8078 Carolejordan. This small, high-albedo inner main-belt asteroid, observed in three long sessions, was found to have synodic rotation period of 3.0540(4) h, differing from the sole known report: a tentative estimate of 3.5 h (Oey and Groom, 2019). A *G* value of 0.30 slightly improved the Fourier fit over the default value of 0.15; RMS error was 15 millimagnitudes.

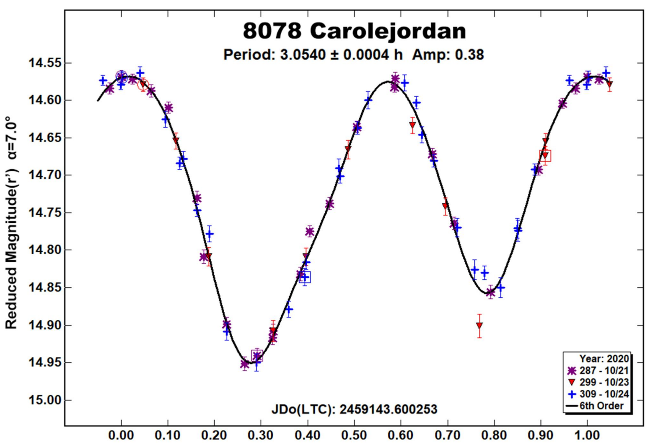

The 2019 period report was offered as only a tentative solution since the asteroid was a target of opportunity and its lightcurve was partial; that 3.5 h estimate does not appear in our period spectrum.

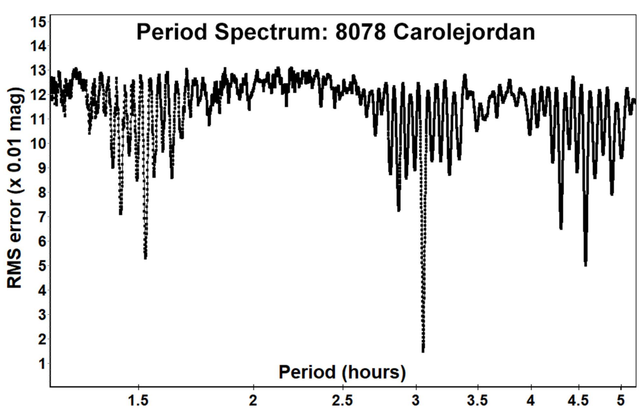

10221 Kubrick. We found the synodic rotation period of this faint Vestoid asteroid to be 11.070(2) h and its amplitude to be 0.20 magnitude, in agreement with the sole known survey estimate of 11.0(2) h and 0.19 magnitude (Chang et al, 2019). A *G* value of 0.38 gave markedly better Fourier fits than did *G* = 0.15; RMS error was 30 millimagnitudes.

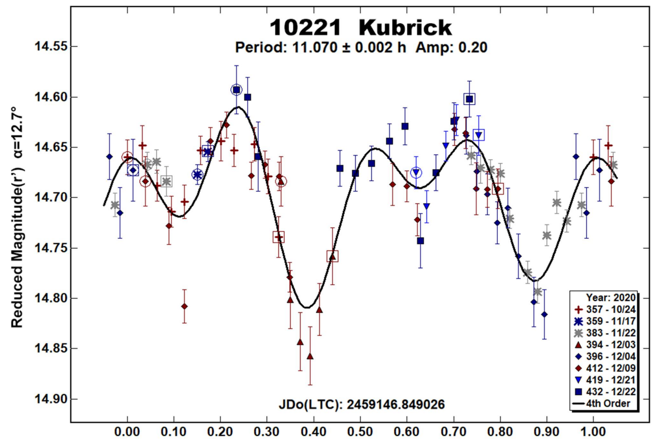

Though the amplitude is modest and the lightcurve is complex in shape, the period spectrum does support the bimodal period proposed, though observational noise allows for an alternative monomodal period of 5.54 h, especially given the relatively small amplitude (Harris et al, 2014).

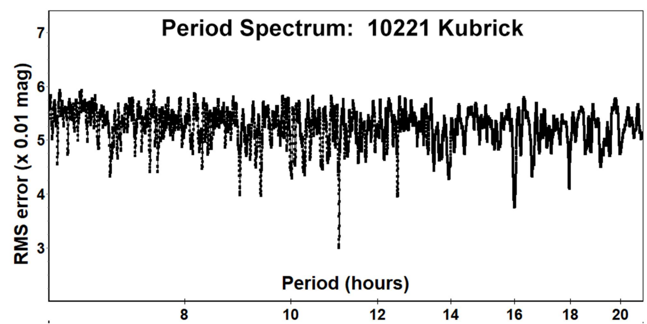

(21787) 1999 SG4. This Eunomia-family asteroid was detected in images targeting 722 Frieda and then was followed in its own right. No previous period or lightcurves are known; we measured a synodic period of 2.9388 (4) h. A *G* value of 0.35 gave far superior Fourier fits to those using *G* = 0.15; RMS error is 26 millimagnitudes.

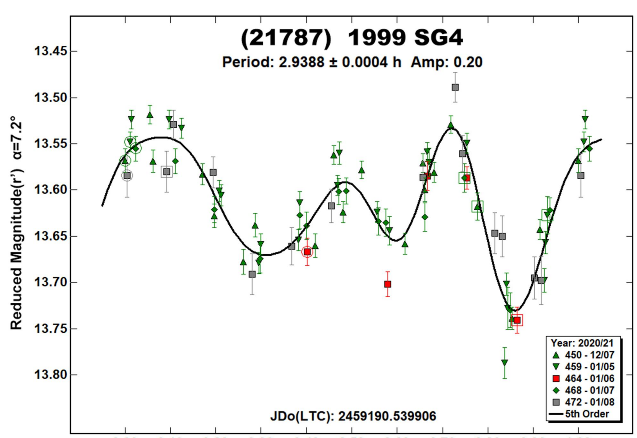

The short period and advantageous declination allowed rapid elimination of alias periods despite Sloan r' magnitudes near 17.

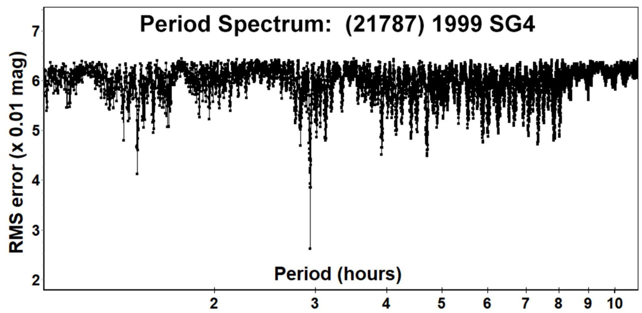

26858 Misterrogers. This Mars-crosser has only a single previous lightcurve and synodic period report of 8.065 h (Skiff, 2019). Our 2020 observations during seven nights over five weeks simply could not discriminate between periods near 6 and 8 hours, which are aliases by one period per 24 hours. RMS error was 12 millimagnitudes.

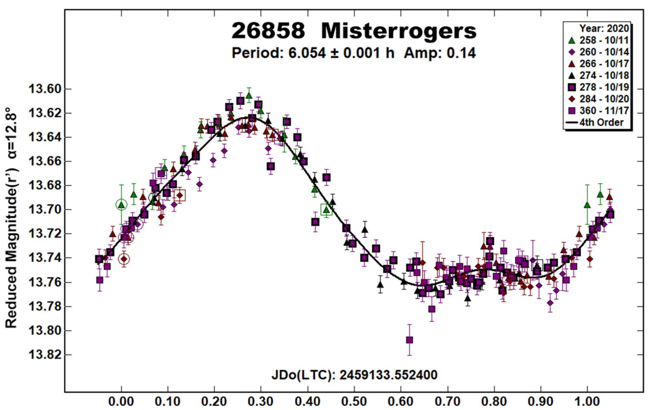

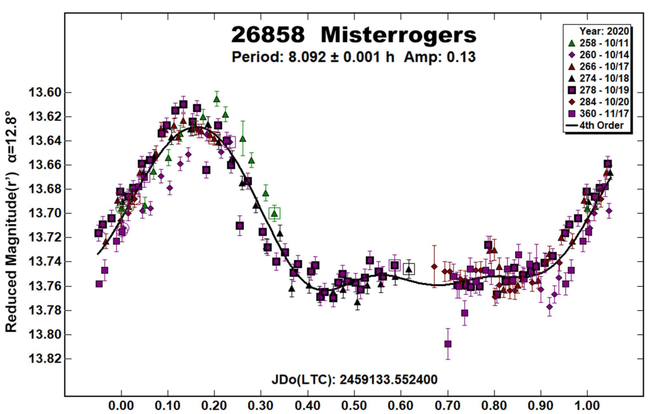

The period spectrum slightly favors the 6.054(1) h over the 8.092(1) h solution, but either solution might well have been accepted if considered in isolation, which serves as a reminder to continue observing until the aliasing symmetry is broken or until one concludes that no additional sessions could do so. This observing campaign falls in the latter case due to several unfortunate conditions: the closeness of both candidate periods to an integral fraction of 24 hours, which guarantees that aliases will emerge; the lightcurve's having only a single feature; and session lengths being limited by the target's declination.

This asteroid's orbit keeps it near the plane of the earth's equator, so it is unclear that an unambiguous rotational period for 26858 Misterrogers could ever be decided by any number of observations from a single terrestrial site. A multi-longitudinal cooperative study is encouraged.

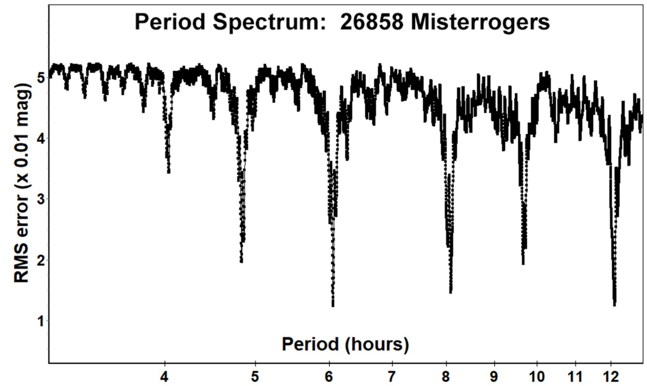

(49125) 1998 SB22. This Vestoid-family asteroid was detected in images targeting asteroid 3061 Cook and then was followed in its own right. No previous lightcurves or synodic period reports are known to the author. The present observations yield a period of 5.9676(8) h despite the RMS error of 77 millimagnitudes. A *G* of 0.40 markedly improved the Fourier fit vs the default *G* of 0.15.

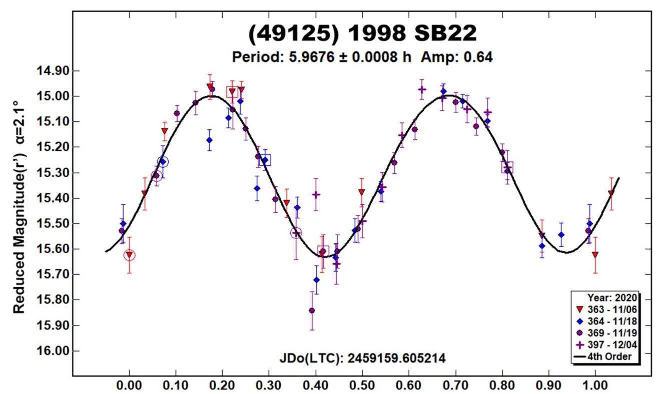

As with 26858 Misterrogers described above, the period is close to an integer fraction of 24 hours, and sessions lengths were limited by an unfavorable declination. However, for (49125) 1998 SB22 the bimodal lightcurve shape and higher amplitude allow for a confident preference for the solution near 6 hours relative to those of 8 and 9 hours, despite their similar RMS errors: the 8- and 9-hour solutions are trimodal and not of reasonable lightcurve shape.

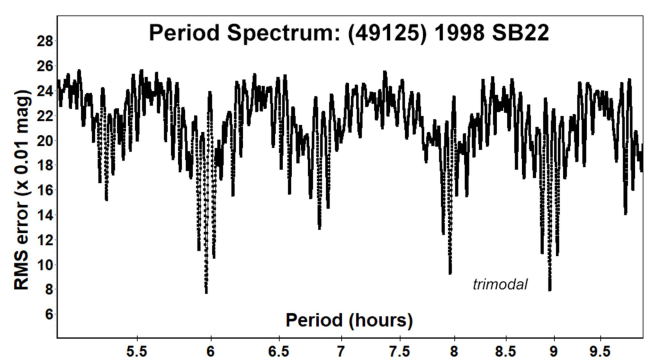

Acknowledgements

The author thanks the authors of the ATLAS paper (Tonry et al, 2018) and the catalog's numerous contributors for providing without cost the ATLAS refcat2 release catalog and its detailed technical descriptions.

This project's computations make extensive use of the python language interpreter and of several supporting packages (notably: pandas, ephem, matplotlib, requests, astropy, and statsmodels), all provided without cost, and without which this work would have been infeasible.

References

Aznar Macias, A.; Carreño Garcerán, A.; Arce Mansego, E.; Brines Rodriguez, P.; Lozano de Haro, J.; Fornas Silva, A.; Fornas Silva, G.; Mas Martinez, V.; Rodrigo Chiner, O.; Herrero Porta, D. (2016). "Twenty-one Asteroid Lightcurves at Group Observadores de Asteroides (OBAS): Late 2015 to Early 2016." *Minor Planet Bull.* **43**, 257-263.

Behrend, R. (2002web, 2004web, 2005web, 2012web, 2013web, 2019web). Observatoire de Geneve web site. *http://obswww.unige.ch/~behrend/page_cou.html*

Benishek, V. (2018). "Lightcurve and Rotation Period Determinations for 29 Asteroids." *Minor Planet Bull.* **45**, 82-91.

Chang, C.-K.; Lin, H.-W.; Ip, W.-H.; Chen, W.-P.; Yeh, T.-S.; Chambers, K.C.; Magnier, E.A.; Huber, M.E.; Flewelling, H.A.; Waters, C.Z.; Wainscoat, R.J.; Schultz, A.S.B. (2019). "Searching for Super-fast Rotators Using the Pan-STARRS 1." *Astrophys. J. Suppl. Series* **241**, 6.

Ditteon, R.; West, J.; McDonald, B. (2011). "Asteroid Lightcurve Analysis at the Oakley Southern Sky Observatory: 2011 January thru April." *Minor Planet Bull.* **38**, 214-217.

Ditteon, R.; Adam, A.; Doyel, M.; Gibson, J.; Lee, S.; Linville, D.; Michalik, D.; Turner, R.; Washburn, K. (2018). "Lightcurve Analysis of Minor Planets Observed at the Oakley Southern Sky Observatory: 2016 October - 2017 March." *Minor Planet Bull.* **45**, 13-16.

Dose, E. (2020a). "A New Photometric Workflow and Lightcurves of Fifteen Asteroids." *Minor Planet Bull.* **47**, 324-330.

Dose, E. (2020b). "Lightcurves of Nineteen Asteroids." *Minor Planet Bull.* **48**, 69-76.

Ďurech, J.; Hanuš, J.; Oszkiewicz, D.; Vančo, R. (2016). "Asteroid models from the Lowell photometric database." *Astron. Astrophys.*, **587**, A48.

Hanuš, J.; Ďurech, J.; Brož, M.; Marciniak, A.; Warner, B.D.; Pilcher, F.; Stephens, R.; Behrend, R.; Carry, B.; and 111 coauthors. (2013). "Asteroids' physical models from combined dense and sparse photometry and scaling of the YORP effect by the observed obliquity distribution." *Astron. Astrophys.* **551**, A67.

Harris, A.W.; Young, J.W.; Scaltriti, F.; Zappala, V. (1984). "Lightcurves and phase relations of the asteroids 82 Alkmene and 444 Gyptis." *Icarus* **57**, 251-258.

Harris, A.W.; Pravec, P.; Galád, A.; Skiff, B.A.; Warner, B.D.; Világi, J.; Gajdoš, Š.; Carbognani, A.; Hornoch, K.; Kušnirák, P.; Cooney, W.R.; Gross, J.; Terrell, D.; Higgins, D.; Bowell, E.; Koehn, B.W. (2014). "On the maximum amplitude of harmonics on an asteroid lightcurve." *Icarus* **235**, 55-59.

Hess, K.; Ditteon, R. (2016). "Asteroid Lightcurve Analysis at the Oakley Southern Sky Observatory: 2015 February." *Minor Planet Bull.* **43**, 87.

Mas, V.; Fornas, G.; Lozano, J.; Rodrigo, O.; Fornas, A.; Carreño, A.; Arce, E.; Brines, P.; Herrero, D. (2018). "Twenty-one Asteroid Lightcurves at Asteroids Observers (OBAS) - MPPD: Nov 2016 - May 2017." *Minor Planet Bull.* **45**, 76-82.

Oey, J.; Világi, J.; Gajdoš, Š.; Kornoš, L.; Galád, A. (2007). "Light Curve Analysis of 8 Asteroids from Leura and Other Collaborating Observatories." *Minor Planet Bull.* **34**, 81-83.

Oey, J.; Groom, R. (2019). "Lightcurve Analysis of Asteroids from BMO and DRO in 2016. II." *Minor Planet Bull.* **46**, 119-125.

Olguín, L.; Saucedo, J.C.; Loera-González, P.; Contreras, M.E.; Valdés, J.R.; Guichard, J.; López-González, R.; Michimani-García, J.; Cerdán-Hernández, G.; Schuster, W.J.; Valdés-Sada, P.; Núñez-López, R.; Ayala-Gómez, S.A. (2020). "The Mexican Asteroid Photometry Campaign." *Minor Planet Bull.* **47**, 340-342.

Pál, A.; Szakáts, R.; Kiss, C.; Bódi, A.; Bognár, Z.; Kalup, C.; Kiss, L.L.; Marton, G.; Molnár, L.; Plachy, E.; Sárneczky, K.; Szabó, G.M.; Szabó, R. (2020). "Solar System Objects Observed with TESS - First Data Release: Bright Main-belt and Trojan Asteroids from the Southern Survey." *Astrophys. J. Suppl. Series* **247**, 1.

Pilcher, F.; Benishek, V. (2009). "Period Determinations for 634 Ute and 805 Hormuthia." *Minor Planet Bull.* **36**, 29-30.

Polakis, T. (2018). "Lightcurve Analysis for Fourteen Main-Belt Minor Planets." *Minor Planet Bull.* **45**, 347-352.

Polakis, T. (2019). "Photometric Observations of Seventeen Minor Planets." *Minor Planet Bull.* **46**, 400-406.

Polakis, T. (2020). "Photometric Observations of Seven Minor Planets." *Minor Planet Bull.* **48**, 23-25.

Pravec, P. (2018web). Ondrejov Asteroid Photometry Project web site. *http://www.asu.cas.cz/~ppravec/neo.htm*

Singh, A.; Sackalosky, C.; Sefik, Y.; Yates, E.; Moore, C.; Pagan, A.; Malwitz, A. (2020). "Lightcurve for Asteroid 4717 Kaneko." *Minor Planet Bull.* **47**, 74.

Skiff, B.A.; McLelland, K.P.; Sanborn, J.J.; Pravec, P.; Koehn, B.W.; Bowell, E. (2019). "Lowell Observatory Near-earth Asteroid Photometric Survey (NEAPS): Paper 3." *Minor Planet Bull.* **46**, 238-265.

Stephens, R.D. (2002). "Photometry of 866 Fatme, 894 Erda, 1008 Demeter, and 3443 Letsungdao." *Minor Planet Bull.* **29**, 2-3.

Tonry, J.L.; Denneau, L.; Flewelling, H.; Heinze, A.N.; Onken, C.A.; Smartt, S.J.; Stalder, B.; Weiland, H.J.; Wolf, C. (2018). "The ATLAS All-Sky Stellar Reference Catalog." *Astrophys. J.* **867,** A105, 1-16.

Warner, B.D. (2003). "Lightcurve analysis for asteroids 607 Jenny, 1177 Gonnessia 4440 Tchantches, 4896 Tomoegozen, and (4995) 1984 QR." *Minor Planet Bull.* **30**, 33-35.

Warner, B.D. (2008). "Asteroid Lightcurve Analysis at the Palmer Divide Observatory: June - October 2007." *Minor Planet Bull.* **35**, 56-60.

Warner, B.D.; Harris, A.W.; Pravec, P. (2009). "The asteroid lightcurve database." *Icarus*, **202**, 134-146. Updated 2020 August. *http://www.minorplanet.info/lightcurvedatabase.html*

Warner, B.D. (2018). *MPO Canopus* Software, version 10.7.12.9. BDW Publishing. *http://www.bdwpublishing.com*

Waszczak, A.; Chang, C.-K.; Ofek, E.O.; Laher, R.; Masci, F.; Levitan, D.; Surace, J.; Cheng, Y.-C.; Ip, W.-H.; Kinoshita, D.; Helou, G.; Prince, T.A.; Kulkarni, S. (2015). "Asteroid Light Curves from the Palomar Transient Factory Survey: Rotation Periods and Phase Functions from Sparse Photometry." *Astron. J.* **150**, 3.

LIGHTCURVES AND ROTATION PERIODS OF 67 ASIA, 74 GALATEA, 356 LIGURIA, 570 KYTHERA, 581 TAUNTONIA, 589 CROATIA, AND 605 JUVISIA

Frederick Pilcher
Organ Mesa Observatory (G50)
4438 Organ Mesa Loop
Las Cruces, NM 88011 USA
fpilcher35@gmail.com

(Received: 2021 Jan 14)

Synodic rotation periods and amplitudes are found for 67 Asia: 15.855 ± 0.002 h, 0.32 ± 0.02 mag; 74 Galatea: 17.266 ± 0.001 h, 0.06 ± 0.01 mag; 356 Liguria: 31.690 ± 0.002 h, 0.14 ± 0.01 mag; 570 Kythera: 8.117 ± 0.001 h, 0.09 ± 0.01 mag; 581 Tauntonia: 24.994 ± 0.002 h, 0.10 ± 0.01 mag; 589 Croatia: 24.932 ± 0.001 h, 0.25 ± 0.01 mag; 605 Juvisia: 15.844 ± 0.001 h, 0.18 ± 0.01 mag.

Observations to obtain the data used in this paper were made at the Organ Mesa Observatory with a 0.35-m Meade LX200 GPS Schmidt-Cassegrain (SCT) and SBIG STL-1001E CCD. Exposures were 60 seconds, unguided, with a clear filter except where otherwise noted. Photometric measurement and lightcurve construction are with *MPO Canopus* software. To reduce the number of points on the lightcurves and make them easier to read, data points have been binned in sets of 3 with a maximum time difference of 5 minutes. For each target a split halves plot of the double period has been plotted that shows the two halves of the double period are very nearly the same. Therefore, the double period may be ruled out for each target. Although not shown in this paper, these plots are available from the author on request.

67 Asia. The Asteroid Lightcurve Database (Warner et al, 2009) states a secure period of 15.853 hours based on six independent period determinations all within 0.05 hours of the preferred value. A lightcurve based on new observations on four nights 2020 Nov. 6-17 at phase angles from 6.7º to 11.8º provide an excellent fit to a period 15.852 ± 0.001 h, amplitude 0.32 ± 0.02 mag. These four sessions were timed to obtain full phase coverage of the double period, whose split halves plot, not presented, shows a near perfect overlap of the two halves. The double period may be safely ruled out.